

Discrimination of Parkinsonian tremor from essential tremor by implementation of a wavelet-based soft-decision technique on EMG and accelerometer signals

A. Hossen^{a,*}, M. Muthuraman^b, J. Raethjen^c, G. Deuschl^c, U. Heute^b

^a Department of Electrical and Computer Engineering, Sultan Qaboos University, P.O. Box 33, Al-Khoud, 123 Muscat, Oman

^b Institute for Circuit and System Theory, Faculty of Engineering, University of Kiel, D-24143 Kiel, Germany

^c Department of Neurology, University of Kiel, Schittenhelmstraße 10, D-24105 Kiel, Germany

1. Introduction

Essential tremor (ET) and the tremor in Parkinson's disease (PD) are the two most common pathological tremor forms encountered in clinical neurology [1]. Where ET is a relatively benign disease with the tremor being the main symptom, PD is a progressive neuro-degenerative disorder in the course of which other disabling neurological deficits develop. Differential diagnosis between the two tremors is usually achieved clinically. But there is a certain overlap in the clinical presentation between the two diseases that can make the differentiation on purely clinical grounds difficult [2]. In such unclear cases, functional imaging of the dopaminergic deficit as the hallmark of PD is considered the diagnostic gold standard [3,4]. However, this requires SPECT (Single Photon Emission Computer Tomography)-technology, injection of a radioactivity-labeled dopamine transporter ligand into the patients (DAT-Scan), and needs a considerable amount of time. Thus more readily available and easier diagnostic tests are desirable [5]. Spectral analysis of

tremor time-series recorded by accelerometry and surface EMG is a common approach [6]. It has proven useful to distinguish between physiological and pathological tremor [7] but is not superior to the clinical assessment in the distinction of ET from PD in its present form [8].

Therefore methods beyond the standard spectral analysis of the recorded tremor time-series have been applied in an attempt to find a way to safely separate ET and PD [9–14].

These methods seemed to have reasonable diagnostic yields: an almost complete separation between 25 PD and 15 ET subjects was obtained on the basis of the asymmetric decay of the auto-correlation function in a time-series analysis [9]. However, this approach does not investigate the frequency domain and it is not clear, if it is equally successful in different and larger samples. A method of long-term EMG recording was proved to be suitable for the separation of PD tremor and ET [10]. But this is more time consuming and cumbersome to patients and doctors as it entails more than one visit and longer recording times also outside the laboratory [12]. We hypothesize that the power spectra of short (30 s) EMG and accelerometer time-series recorded in a laboratory setting carry more information in the different frequency bands and this information from the frequency domain could be utilized for the differential diagnosis between ET and PD tremor.

A different approach of spectral analysis is suggested in this paper. This approach is based on a soft-decision wavelet-

* Corresponding author. Tel.: +968 24141303; fax: +968 24413454.

E-mail addresses: abhossen@squ.edu.om (A. Hossen),

mm@tf.uni-kiel.de (M. Muthuraman), j.raethjen@neurologie.uni-kiel.de (J. Raethjen), g.deuschl@neurologie.uni-kiel.de (G. Deuschl), uh@tf.uni-kiel.de (U. Heute).

Table 1

Trial data-size, age, gender, and disease duration distribution of both PD and ET subjects.

	PD	ET
Number of patients	19	21
Mean age (range)	64.54 (40–90) years	63.24 (27–94) years
Gender (male/female)	11/8	12/9
Mean disease duration	16.4 years	34 years

Table 2

Test data-size, age, gender, and disease duration distribution of both PD and ET subjects.

	PD	ET
Number of patients	20	20
Mean age (range)	68.22 (52–85) years	64.52 (32–86) years
Gender (male/female)	12/8	11/9
Mean disease duration	15.3 years	29 years

decomposition technique, and it succeeds in obtaining 85% accuracy of discrimination of ET from PD.

The organization of the paper is as follows: in Section 2, both the trial data and test data are described. Section 3 contains the main idea of the soft-decision wavelet-based technique with its implementation on trial data. The results of implementation on test data and discussion of the results are given in Section 4. Section 5 contains conclusions and some remarks concerning the follow-up of the presented work.

2. Data acquisition

2.1. Subjects

In this study, 39 PD and 41 ET subjects were analyzed, respectively. All patients are suffering from a moderate to severe postural tremor. This postural tremor could not be differentiated on clinical grounds with respect to frequency, amplitude, or other features. The data is divided into two sets and to be used for training (trial set) and for testing (test set), respectively. The features are to be obtained from the training set and the discrimination algorithm is to be tested for performance evaluation on the test set. The mean age, sex and disease duration of the PD patients were compared with the ET patients for the trial and test data in Tables 1 and 2. All patients gave informed consent, and the study was approved by the local ethics committees at the University of Kiel.

It is important to mention at this stage that the data size is marginal (not large enough) to yield general results and this will even limit the consistency test methods that can be used along with such a marginal data size.

2.2. Tremor recording

The settings in which the data from both the PD and ET patients were recorded, were almost identical. The patients belonging to both groups were comfortably seated in an armchair with their forearm supported by the arm rests. Postural tremor was recorded from the more affected side, while subjects extended their hands and fingers actively to a 0° position with the resting forearm. This posture was held against gravity, and in this condition the tremor was recorded for a period of 30 s. A piezoelectric accelerometer of about 2 g was fixed to the dorsum of the more affected hand in the middle of the third metacarpal bone, and bipolar surface EMG recordings with silver–silver–chloride electrodes from forearm flexors (EMG1) and extensors (EMG2) were taken. EMG electrodes were fixed close to the motor points of the ulnar part of the hand extensor and flexor muscles of the forearm, thereby pref-

erentially recording the extensor and flexor carpi-ulnaris muscles. All data were sampled at 800 Hz. The EMG was band-pass filtered between 50 and 350 Hz and full-wave rectified. The relatively high sampling frequency was useful for the EMG recordings as within the bursts there are frequency components up to 350 Hz and can only be fully picked up with such a sampling frequency to satisfy the Nyquist theorem.

3. Data analysis method

The spectral-analysis technique applied in the following is based on a specific variant of the so-called sub-band decomposition soft-decision technique [15]. The wavelet-based soft-decision technique is introduced in [16] with an application of wavelet filters instead of the Haar filters used in the conventional sub-band technique. The basis of the wavelet-based technique is to be briefly explained in the following subsection.

3.1. Wavelet-decomposition

The wavelet-decomposition starts by filtering the input signal $x(n)$ of length N by low-pass filters (LPF) and high-pass filters (HPF) and then down-sampling by a factor of 2 to produce both the “approximation” $a(n)$ and the “details” $d(n)$. Assuming that Haar filters are used, then $a(n)$ and $d(n)$ can be obtained by:

$$a(n) = \frac{1}{\sqrt{2}} [x(2n) + x(2n + 1)] \quad (1a)$$

$$d(n) = \frac{1}{\sqrt{2}} [x(2n) - x(2n + 1)] \quad (1b)$$

If it is known that the energy is concentrated in one of the bands, the computation process could be applied in that band and stopped in the other one to reduce complexity and save processing time. The decomposed bands could also be decomposed further into low frequency and high-frequency sub-bands using the same filters. The process of selecting one decomposition path out of the full decomposition is called hard-decision algorithm [15]. The band selection is established by an energy comparison between the low- and high-frequency subsequences $a(n)$ and $d(n)$:

$$B = \sum_{n=0}^{(N/2)-1} (a(n))^2 - (d(n))^2 \quad (2)$$

According to the sign of B , the decision is taken: if B is positive, the low-frequency band $a(n)$ is considered, and if B is negative, the high-frequency band $d(n)$ is considered. Since we are not interested in the value of B , but only in its sign, Eq. (2) can be simplified to the approximation:

$$\text{sgn}(B) = \text{sgn} \sum_{n=0}^{(N/2)-1} |a(n)| - |d(n)|. \quad (3)$$

Energy comparison and band selection are repeated at each decomposition stage; this results in following one decomposition path and narrowing down the estimate of the dominant frequency range of the original sequence.

A useful modification of the hard-decision algorithm is to perform full decomposition in each stage to a specified number of times and assign a “probability measure” that reflects the energy in each decomposed band. This process is called the soft-decision algorithm [15] and found useful in estimating the approximate power-spectral density (PSD) using different wavelet filters [16] in spectral analysis. The soft-decision method has been implemented successfully due to its simplicity and good spectral resolution advantage in many biomedical signal-processing applications, e.g.,

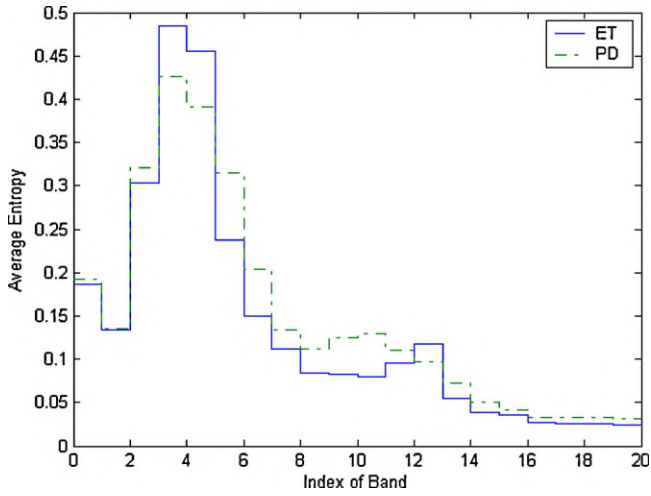


Fig. 1. The average power-entropy plots for both ET and PD cases of trial records (accelerometer).

for the heart-rate variability signal in obstructive sleep apnea or for congestive heart failure [17–19]. The complete procedure for estimating the PSD of the decomposed sub-bands [16] is listed in Appendix A.

3.2. Implementation on trial data

The soft-decision algorithm is implemented on the training data using Daubechies (db4) wavelet filters with $m=8$ decomposition stages, which results in 256 frequency bands. The PSD (the probability values) and the entropies of the 256 bands are obtained for each PD record and ET record. An average power-entropy plot is derived for both diagnostic groups (PD or ET) by averaging the probability values of counterpart bands in each case for each signal out of the three used signals (accelerometer, EMG1 and EMG2). The average power-entropy plots of the 21 ET records and the 19 PD records are shown in Figs. 1–3 for the first 20 bands up to 31.25 Hz for the three different signals, respectively. Figs. 1–3 represent average results and can be considered as standard plots for ET and PD. Frequencies above 31.25 Hz are not considered in our algorithm as both ET and PD tremor frequencies are below 31.25 Hz [6,9]. The number of bands (256) was selected to have good resolution of the estimated power-spectral density. Other than (db4) wavelet filters

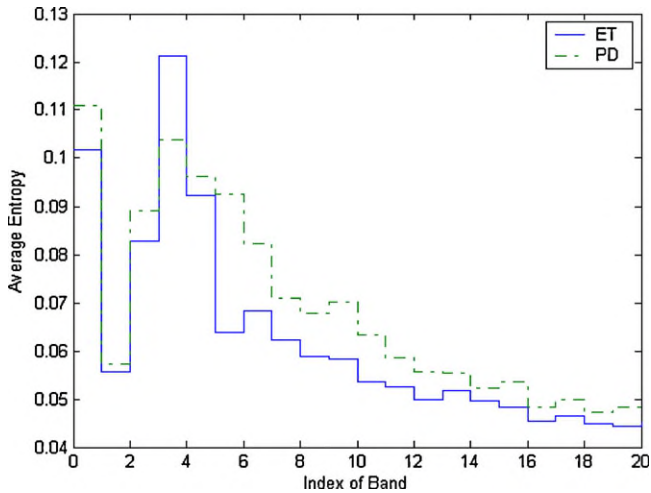


Fig. 2. The average power-entropy plots for both ET and PD cases of trial records (EMG1).

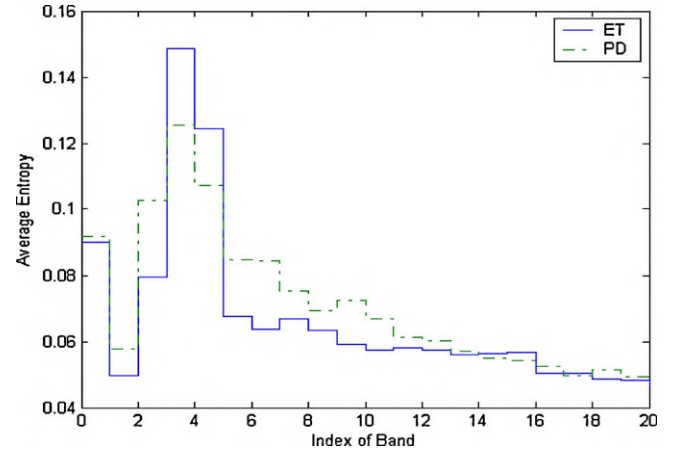


Fig. 3. The average power-entropy plots for both ET and PD cases of trial records (EMG2).

have been also used but no better results are obtained, so results of db4 filters are kept only in the paper due to the simplicity of db4 filters.

3.3. Classification performance

A classifier is a parameter or a variable, with a suitable optimal threshold, that is used in a classification algorithm. In this study, only binary classification is considered, e.g., classification between two different cases termed “positive case” (PD) and “negative case” (ET). The performance of a classifier is evaluated by three main metrics: specificity, sensitivity, and accuracy, as follows [20]:

$$\text{Specificity (\%)} = \frac{\text{TN}}{\text{TN} + \text{FP}} \cdot 100 \quad (4)$$

$$\text{Sensitivity (\%)} = \frac{\text{TP}}{\text{TP} + \text{FN}} \cdot 100 \quad (5)$$

$$\text{Accuracy (\%)} = \frac{\text{TP} + \text{TN}}{T} \cdot 100 \quad (6)$$

where the entities in the above equations are: (TN (true negatives), TP (true positives), FN (false negatives), FP (false positives)), and T is the total number of data under test.

Table 3
Classification results of test data based on first 20 bands.

EMG2		EMG1		Accelerometer		Band number
PD	ET	PD	ET	PD	ET	
9	13	9	16	9	6	B1
9	13	9	16	9	14	B2
9	17	8	16	10	16	B3
11	7	11	7	9	13	B4
12	8	9	12	10	10	B5
13	16	12	16	12	9	B6
8	14	11	13	13	9	B7
11	14	14	14	11	9	B8
11	15	14	11	10	8	B9
10	15	10	15	10	8	B10
11	11	14	17	11	11	B11
6	13	12	10	9	8	B12
11	12	13	14	10	10	B13
11	10	13	12	12	11	B14
12	8	14	14	7	10	B15
12	7	12	8	10	9	B16
9	10	13	11	14	10	B17
13	10	11	14	8	10	B18
8	12	12	13	7	10	B19
10	11	10	14	11	10	B20

Table 4
Results based on different bands from different signals using test data set.

Classification based on	Band number	Correct ET subjects	Correct PD subjects
Accelerometer signal	B17	4, 5, 6, 7, 8, 9, 11, 15, 17, 18	1, 3, 5, 6, 7, 8, 11, 12, 13, 16, 17, 18, 19, 20
EMG1	B11	1, 2, 5, 6, 7, 8, 9, 10, 11, 13, 14, 15, 16, 17, 18, 19, 20	2, 3, 4, 5, 8, 9, 11, 12, 14, 15, 16, 17, 18, 20
EMG2	B6	1, 2, 3, 4, 6, 8, 9, 10, 13, 14, 15, 16, 17, 18, 19, 20	2, 3, 4, 5, 6, 9, 11, 14, 15, 16, 17, 19, 20
Voting		1, 2, 4, 5, 6, 7, 8, 9, 10, 11, 13, 14, 15, 16, 17, 18, 19, 20	2, 3, 4, 5, 6, 8, 9, 11, 12, 14, 15, 16, 17, 18, 19, 20

Table 5
Performance factors for the three signals obtained from training data.

Case	CFET	CFPD
Accelerometer	0.3172	0.4448
EMG1	0.1175	0.1558
EMG2	0.1249	0.1516

Table 6
Performance analysis of the technique obtained from test data.

Case	Specificity (%)	Sensitivity (%)	Accuracy (%)
Accelerometer	55	60	57.5
EMG1	85	65	75
EMG2	80	75	77.5

Specificity indicates the ability of a classifier to detect negative cases, i.e., the ET cases. Sensitivity represents the ability of a classifier to detect the positive cases, i.e., the PD cases. Accuracy represents the overall performance of a classifier. It indicates the percentage of correctly classified positive and negative cases among the total number of cases.

4. Results

In order to discriminate ET from PD based on power-entropy results, a blind search has been implemented to find any band or combination of bands that can lead to clear or good discrimination between the two groups. By a blind search, we mean a search in which no a-priori information is known about any relation between tremors and frequency bands. This means that all frequency bands from B1 to B20 (up to 31.25 Hz) are given the same priority in our search about the discrimination features.

4.1. Classification based on single band

The average entropy of each band from (B1–B20) for all ET and PD training data is computed respectively for all three signals. In the test stage, the entropy of each band is computed for the data under test and a decision is made to classify the signal as ET or PD if its entropy of that calculated band is close to the corresponding band of the average training ET or PD, respectively. Table 3 shows the numbers TN and TP of correctly classified ET and PD cases, respectively, out of $T=20$ subjects under test from each category. We can notice that the best result is obtained with EMG1 using band 11, with a specificity of $17/20$ (85%), sensitivity of $14/20$ (70%), and accuracy of $31/40$ (77.5%).

Table 7
Results based on sum of entropy of two bands from different signals.

Classification based on	Band number	Correct ET subjects	Correct PD subjects
Accelerometer signal	B6 + B11	4, 5, 6, 7, 8, 9, 11, 14, 15, 17, 18	2, 4, 6, 7, 8, 11, 14, 16, 17, 18, 19, 20
EMG1	B6 + B11	1, 2, 3, 6, 7, 8, 9, 10, 11, 13, 14, 15, 16, 17, 18, 19, 20	2, 3, 4, 5, 8, 9, 10, 11, 14, 15, 17, 18, 20
EMG2	B6 + B11	1, 2, 3, 4, 5, 6, 9, 10, 13, 14, 15, 16, 17, 18, 19, 20	2, 3, 4, 5, 6, 8, 9, 11, 14, 15, 16, 17, 18, 19, 20
Voting		1, 2, 3, 4, 5, 6, 7, 8, 9, 10, 11, 13, 14, 15, 16, 17, 18, 19, 20	2, 3, 4, 5, 6, 8, 9, 11, 14, 15, 16, 17, 18, 19, 20

4.2. Classification based on different bands from different signals

For each data under test, we compute B17 from the accelerometer signal and B11 from EMG1 signal and B6 from EMG2 signal. The signal under test is classified three times according to the results of the three different bands from the three different signals. A voting between the three classifications is done such that if a signal is classified twice out of three times as ET then it is considered as ET subject, while otherwise it is considered as PD. Table 4 shows the result of such a classification. The numbers listed in each row under ET and PD represent the indexes of the subjects that are correctly classified as ET or PD. The efficiency of the voting step is a specificity of 90%, a sensitivity of 80%, and an accuracy of 85%.

It is important to mention at this stage, that the selection of those three bands is not randomly done, but a blind search has been implemented for all bands to find the best combination of bands from different signals to give the best discrimination result. If we investigate the results of Table 3 and especially for the accelerometer signal, B3 shows better specificity and accuracy results than B17, while B17 has been selected in the combination because it shows better sensitivity results than B3 and gives better accuracy results in the voting step.

4.3. Classification based on the sum of entropy of the same two bands from different signals

A blind search was implemented to find a combination of the same two bands from the three different signals of training set to be used as a classification factor. This blind search leads to a good classification factor (CF) between the two groups, namely, the sum of the power entropies of bands 6 (7.8125–9.375 Hz) and 11 (15.625–17.1875 Hz) averaged over all ET and PD cases, respectively. Values of this classification factor for ET (CFET) and PD (CFPD) for the three different signals are listed in Table 5. By blind search here, we mean that all combinations of two bands have been tried to find the best combination B6 and B11.

The values of CF (sum of power entropies of both bands 6 and 11), is found for each data under test for the three different signals. A final discrimination factor between ET and PD named M is computed as:

$$M = (CF - CFET)^2 - (CF - CFPD)^2 \quad (7)$$

The value of M is a measure of the difference between the squared distances of the data under test from a standard ET factor CFET to those from a standard PD factor CFPD. If the result is negative, this means that the data under test is closer to a standard ET case than to a standard PD case, and hence it is considered as ET (negative case). If the result is positive, this means that the data under test is closer

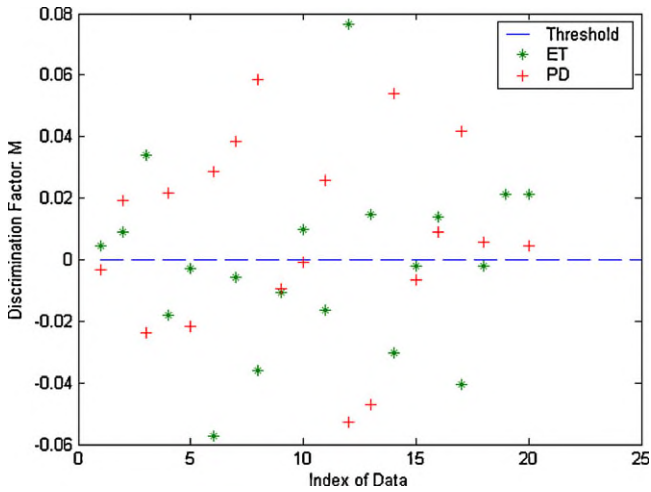


Fig. 4. Values of M for data under test (accelerometer).

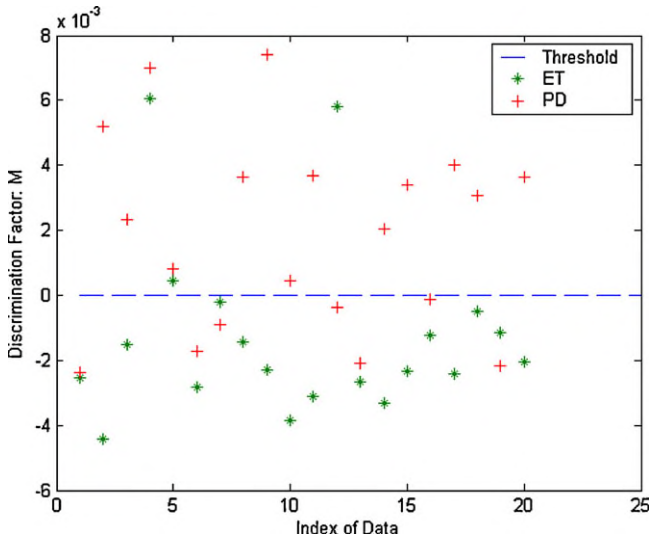


Fig. 5. Values of M for data under test (EMG1).

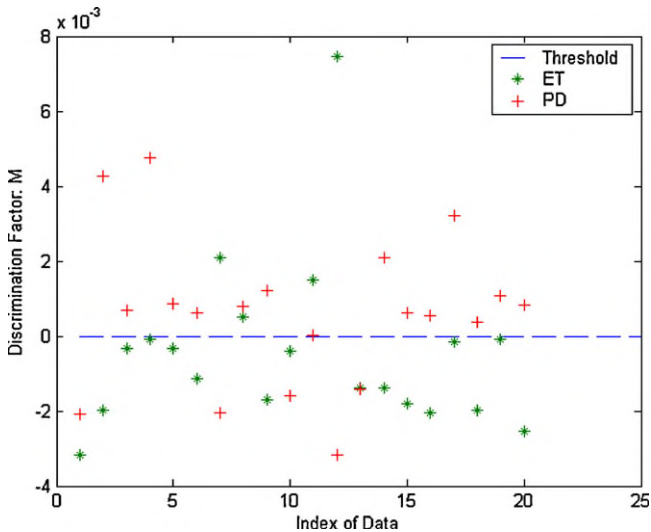


Fig. 6. Values of M for data under test (EMG2).

to a standard PD than to a standard ET, and hence it is considered as PD (positive case). Values of M are plotted for all data under test in Figs. 4–6 for the three different signals, respectively. The threshold value between the two categories, which is the 0 value, is also shown in the figures. The values of the specificity, sensitivity, and accuracy obtained from those figures corresponding to the three signals are listed in Table 6.

Now in addition, a “voting” is used between the three results of Table 6 for each data under test in such a way that, if the data is classified in any category (ET or PD) two times or more, it is considered belonging to that category. Such a voting idea results in a specificity of 95% and a sensitivity of 75% and an accuracy of 85%. Table 7 shows detailed results of this section with the voting results.

To test the consistency of the results with regard to data dependency, a 2-fold cross-validation approach is done, in which the test data set has been used in the trial stage, and the trial data set has been used in the test stage. The classification factors and the performance analysis are listed in Appendix B (Tables B.1 and B.2). A voting is used between the three results of Table B.2. This voting step resulted in a specificity of 95%, a sensitivity of 63%, and an accuracy of 80%. Table B.3 shows detailed results of this part with the voting results. Values of M are plotted for the three signals in Figs. B.1–B.3. Other test methods such as leave-one-out-method have not been used at this stage due to the small size of data.

5. Discussion and conclusions

A complete discrimination system for essential and Parkinson tremors based on the computation of power entropy of wavelet-decomposed spectra using the fast approximate soft-decision technique is implemented and tested on trial and test data obtained from the Department of Neurology of the University of Kiel, Germany. The classification system is complete in the sense of using two sets of data, the first one for training and obtaining threshold values of the classification factor, and the second one for testing the performance of the implemented technique. An accuracy of classification up to 85% is obtained from the test data. The technique uses as a classification factor the sum of power entropies of bands 6 and 11 out of 256 bands estimating the power-spectral density of the accelerometer and EMG signals. The method is computationally simple and could be developed into a supporting test in the clinical differential diagnosis between ET and PD-tremor. However, results from larger numbers of clinically well-defined patients would be desirable before applying our test in a routine clinical setting.

A weighted-voting process between the results of the three signals according to their efficiency in discrimination between ET and PD of the trial set can be also used to discriminate between ET and PD in the test stage. Such a process may be of better results than the normal voting approach applied in this paper, especially if it is used with a larger size of data size.

Given the fact that we only looked at the postural tremor which cannot be distinguished on clinical grounds the present results show a surprisingly good separation between ET and PD selectively looking at specific frequency bands. We show here that a more detailed spectral analysis taking into account frequency bands beyond the actual tremor frequencies is a worthwhile approach in diagnostic clinical neurophysiology of tremors. Interestingly, it was the frequency bands between 7.8125 and 9.375 Hz and 15.625 and 17.1875 Hz that allowed for the best separation between the two common tremors. These bands are very close to the frequency regions in which the first and second harmonic peaks at double and triple the tremor frequency are found. Thus it may be

this common phenomenon of harmonic peaks in higher amplitude tremors that carries differential diagnostic information. This would be in keeping with a previous study showing that nonlinearities in the tremor wave forms (asymmetry) that typically give rise to higher harmonic peaks could separate between ET and PD [9]. It is a common observation that PD patients more regularly show peaks at harmonics of the basic tremor frequency than ET patients. More recently it has also been postulated that the harmonic peaks in PD tremor may not be solely related to waveform asymmetries but also to a second tremor generator at double the frequency [11,21] and it has even been speculated that double the basic tremor frequency is the main central drive resulting in the reciprocal alternating pattern of Parkinsonian tremor in the periphery [22]. These phenomena are not encountered to the same extent in ET patients [23,24] and one may speculate that they are the basis of the differences found in these frequency bands in our present results. However, the frequency band between 8 and 9.5 Hz is slightly lower than the expected 10 Hz first harmonic peak for typical 5 Hz PD tremors and the band between 15.5 and 17 Hz is slightly higher than the expected second harmonic peaks. But we know that the harmonic peaks are typically broader than those at the basic tremor frequency and may well cover also the frequency bands found in the present study. Nevertheless information other than the harmonic peaks may also be carried in these bands and further studies specifically looking at the individual harmonic frequencies are necessary to solve this issue.

Acknowledgements

The support by DAAD (German Academic Exchange Service) through a research scholarship for the first author and the support from the German Research Council (Deutsche Forschungsgemeinschaft, DFG: SFB 855) are gratefully acknowledged.

Appendix A.

A.1. Estimation of power-spectral density

The following procedure is used to estimate the PSD of the decomposed sub-bands [16]:

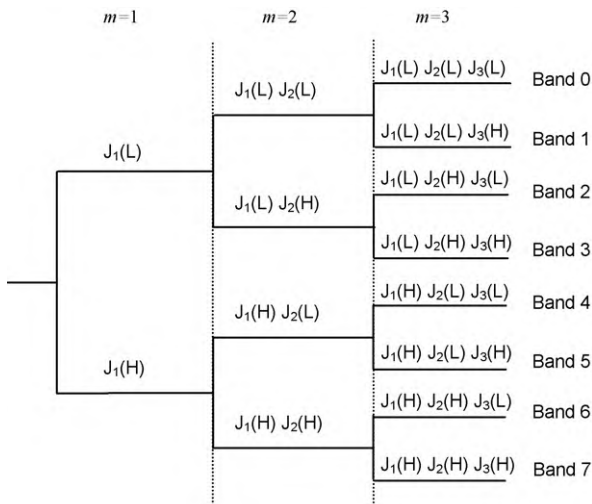


Fig. A.1. PSD estimation by probability assignments for 8 sub-bands ($m=3$ decomposition stages).

1. The wavelet-decompositions are computed for all branches up to a certain stage m to obtain 2^m sub-bands.
2. All estimator results up to stage m are stored, and a probability measure is assigned to each path (i.e., frequency band) to bear the primary information as will be explained in the next steps.
3. If $J(L)$ is the assigned probability of the input signal being primarily low-pass, the number $J(H)=1-J(L)$ is the probability that the signal is primarily high-pass. One simple way to make the probability assignments is to use the ratio of the number of positive comparisons between $|a(n)|$ and $|d(n)|$ in Eq. (3) to the total number of comparisons for a given stage.
4. At the following stage, the resulting estimate can be interpreted as the conditional probability of the new input sequence containing primarily low (high) frequency components, given that the previous branch was predominantly of the low (high)-pass type. Using this reasoning and laws of probability, the assignments for the probability measure of the resulting sub-bands is equal to the product of the previous branch probability and the conditional probability estimated at a given stage. Fig. A.1 shows this step of probability assignment for eight sub-bands (three decomposition stages).
5. The probabilities $P(B_i)$ derived from the estimator outputs, where i is the index of the band, may be interpreted themselves as a coarse measurement of the PSD: the higher the probability value of any band, the higher is its power-spectral content. For m decomposition stages, 2^m bands result. Each band covers $(400/2^m)$ Hz of the signal-spectrum range between 0 and 400 Hz, if the sampling frequency is 800 Hz.
6. The power entropy $H(B_i)$ can be computed from $P(B_i)$ using the following equation for better scaling since the values of probabilities $P(B_i)$ are very small (the sum of the probabilities of all 256 bands equals one):

$$H(B_i) = P(B_i) \log_2 \left(\frac{1}{P(B_i)} \right) \quad (\text{A.1})$$

Appendix B.

See Figs. B.1–B.3 and Tables B.1–B.3.

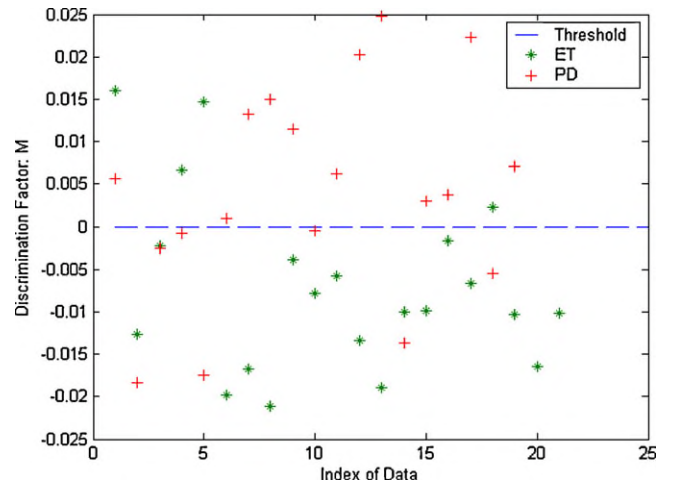


Fig. B.1. Values of M for data under test (accelerometer) (test done on trial data).

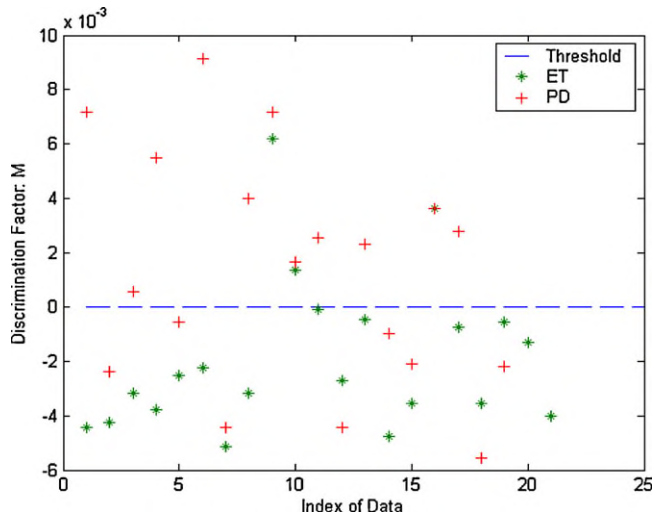


Fig. B.2. Values of M for data under test (EMG1) (test done on trial data).

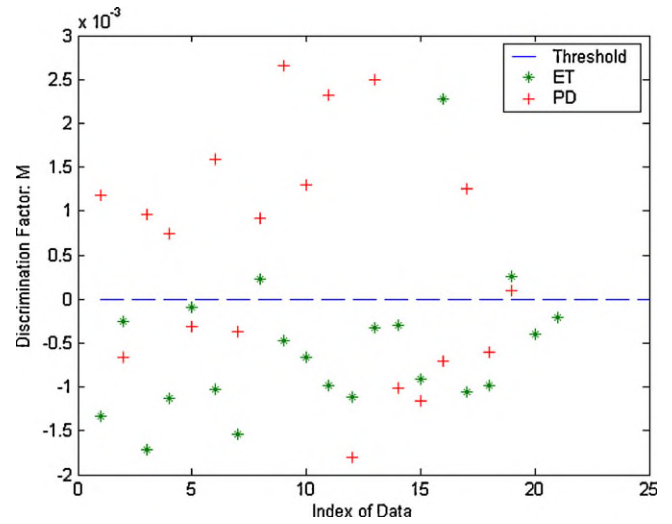


Fig. B.3. Values of M for data under test (EMG2) (test done on trial data).

Table B.1
Classification factors for the three signals obtained from test data.

Case	CFET	CFPD
Accelerometer	0.3775	0.4205
EMG1	0.1201	0.1608
EMG2	0.1299	0.1491

Table B.2
Performance analysis of the technique obtained from trial data.

Case	Specificity (%)	Sensitivity (%)	Accuracy (%)
Accelerometer	81	63	72.5
EMG1	86	58	72.5
EMG2	86	58	72.5

Table B.3
Results based on sum of entropy of two bands from different signals (test done on trial data).

Classification based on	Band number	Correct ET subjects	Correct PD subjects
Accelerometer signal	B6+B11	2, 3, 6, 7, 8, 9, 10, 11, 12, 13, 14, 15, 16, 17, 19, 20, 21	1, 6, 7, 8, 9, 11, 12, 13, 15, 16, 17, 19
EMG1	B6+B11	1, 2, 3, 4, 5, 6, 7, 8, 11, 12, 13, 14, 15, 17, 18, 19, 20, 21	2, 3, 4, 5, 8, 9, 10, 11, 14, 15, 17, 18, 20
EMG2	B6+B11	1, 2, 3, 4, 5, 6, 7, 9, 10, 11, 12, 13, 14, 15, 17, 18, 20, 21	2, 3, 4, 5, 6, 8, 9, 11, 14, 15, 16, 17, 18, 19, 20
Voting		1, 2, 3, 4, 5, 6, 7, 8, 9, 10, 11, 12, 13, 14, 15, 17, 18, 19, 20, 21	1, 3, 4, 6, 8, 9, 10, 11, 13, 16, 17, 19

References

- [1] M.K. Harris, N. Shneyder, A. Borazanci, E. Korniyuchuk, E. Kelley, A. Minagar, Movement disorders, *Med. Clin. North Am.* 93 (2009) 371–388.
- [2] G. Deuschl, P. Bain, M. Brin, Consensus statement of the movement disorder society on tremor, Ad Hoc Scientific Committee, *Mov. Disord.* 13 (Suppl. 3) (1998) 2–23.
- [3] V. Marshall, C.B. Reiningger, M. Marquardt, J. Patterson, D.M. Hadley, W.H. Oertel, H.T. Benamer, P. Kemp, D. Burn, E. Tolosa, J. Kulisevsky, L. Cunha, D. Costa, J. Booi, K. Tatsch, K.R. Chaudhuri, G. Ulm, O. Pogarell, H. Hoffken, A. Gerstner, D.G. Grosset, Parkinson's disease is overdiagnosed clinically at baseline in diagnostically uncertain cases: a 3-year European multicenter study with repeat [(123)I] FP-CIT SPECT, *Mov. Disord.* 24 (2008) 499–507.
- [4] R. Djaldetti, B.I. Nageris, M. Lorberboym, T.A. Treves, E. Melamed, E. Yaniv, [(123)I]-FP-CIT SPECT and oldfation test in patients with combined postural and rest tremor, *J. Neural Transm.* 115 (2008) 469–472.
- [5] A. Antonini, P. Berto, S. Lopatriello, F. Tamma, L. Annemans, M. Chambers, Cost-effectiveness of [(123)I]-FP-CIT-SPECT in the differential diagnosis of essential tremor and Parkinson's disease in Italy, *Mov. Disord.* 23 (2008) 2202–2209.
- [6] G. Deuschl, P. Krack, M. Lauk, J. Timmer, Clinical neurophysiology of tremor, *J. Clin. Neurophysiol.* 13 (1996) 110–121.
- [7] J. Raethjen, M. Lauk, B. Koster, U. Fietzek, L. Friege, J. Timmer, C.H. Lucking, D. Deuschl, Tremor analysis in two normal cohorts, *Clin. Neurophysiol.* 115 (2004) 2151–2156.
- [8] P. Bain, M. Brin, G. Deuschl, R. Elble, J. Jankovic, L. Findley, W.C. Koller, R. Pahwa, Criteria for the diagnosis of essential tremor, *Neurology* 54 (2000) S7.
- [9] G. Deuschl, M. Lauk, J. Timmer, Tremor classification and tremor time series analysis, *CHAOS* 5 (1) (1995) 48–51.
- [10] S. Spieker, C. Jentgens, A. Boose, J. Dichgans, Reliability, specificity and sensitivity of long-term tremor recordings, *Electroencephalogr. Clin. Neurophysiol.* 97 (1995) 326–331.
- [11] N. Sapir, R. Karasik, S. Havlin, E. Simon, J.M. Hausdorff, Detecting scaling in the period of dynamics of multimodal signals: application to Parkinsonian tremor, *Phys. Rev. E* 67 (2003) 1–8, 031903.
- [12] S. Breit, S. Spieker, J.B. Schulz, et al., Long-term EMG recordings differentiate between parkinsonian and essential tremor, *J. Neurol.* 255 (2008) 103–111.
- [13] R.J. Elble, Essential tremor frequency decreases with time, *Neurology* 55 (2000) 1547–1551.
- [14] O. Cohen, S. Pullman, E. Jurewicz, et al., Rest tremor in patients with essential tremor: prevalence, clinical correlates, and electrophysiologic characteristics, *Arch. Neurol.* 60 (2003) 405.
- [15] A. Hossen, U. Heute, Fully adaptive evaluation of SB-DFT, in: *Proceedings of IEEE Int. Symp. on Circuits and Systems*, Chicago, Illinois, 1993.
- [16] A. Hossen, Power spectral density estimation via wavelet decomposition, *Electron. Lett.* 40 (17) (2004) 1055–1056.
- [17] A. Hossen, B. Al-Ghunaimi, M.O. Hassan, Subband decomposition soft decision algorithm for heart rate variability analysis in patients with OSA and normal controls, *Signal Process.* 85 (2005) 95–106.
- [18] A. Hossen, A soft decision algorithm for obstructive sleep apnea patient classification based on fast estimation of wavelet entropy of RRI data, *Technol. Health Care* 3 (2005) 151–165.
- [19] A. Hossen, B. Al-Ghunaimi, A wavelet-based soft decision technique for screening of patients with congestive heart failure, *Biomed. Signal Process. Control* 2 (2007) 135–143.
- [20] R.M. Rangayyan, *Biomedical Signal Analysis: A Case-study Approach*, IEEE Press, NJ, 2001.
- [21] J. Raethjen, R.B. Govindan, M. Muthuraman, et al., Cortical correlates of the basic and first harmonic frequency of Parkinsonian tremor, *Clin. Neurophysiol.* (2009).
- [22] L. Timmermann, J. Gross, M. Dirks, et al., The cerebral oscillatory network of Parkinsonian resting tremor, *Brain* 126 (2003) 199–212.
- [23] B. Hellwig, S. Haussler, B. Schelter, et al., Tremor-correlated cortical activity in essential tremor, *Lancet* 357 (2001) 519–523.
- [24] J. Raethjen, R.B. Govindan, F. Kopper, et al., Cortical involvement in the generation of essential tremor, *J. Neurophysiol.* 97 (2007) 3219–3228.